DISCLAIMER

This report was prepared as an account of work sponsored by an agency of the United States Government. Neither the United States Government nor any agency thereof, nor any of their employees, makes any warranty, express or implied, or assumes any legal liability or responsibility for the accuracy, completeness, or usefulness of any information, apparatus, product, or process disclosed, or represents that its use would not infringe privately owned rights. Reference herein to any specific commercial product, process, or service by trade name, trademark, manufacturer, or otherwise does not necessarily constitute or imply its endorsement, recommendation, or favoring by the United States Government or any agency thereof. The views and opinions of authors expressed herein do not necessarily state or reflect those of the United States Government or any agency thereof. Reference herein to any social initiative (including but not limited to Diversity, Equity, and Inclusion (DEI); Community Benefits Plans (CBP); Justice 40; etc.) is made by the Author independent of any current requirement by the United States Government and does not constitute or imply endorsement, recommendation, or support by the United States Government or any agency thereof.

INL/EXT-21-64594

Iodine Sorption on AgZ-PAN

September 2021

Nick Soelberg, Amy Welty, Sam Thomas

Idaho National Laboratory

INL is a U.S. Department of Energy National Laboratory operated by Battelle Energy Alliance, LLC

INL/EXT-21-64594

Iodine Sorption on AgZ-PAN

Nick Soelberg, Amy Welty, Sam Thomas

September 2021

Idaho National Laboratory
Idaho Falls, Idaho 83415

http://www.inl.gov

Prepared for the
U.S. Department of Energy
Office of Nuclear Energy
Under DOE Idaho Operations Office
Contract DE-AC07-05ID14517

Page intentionally left blank

SUMMARY

The Department of Energy (DOE) Nuclear Fuel Cycle and Supply Chain Program Material Recovery and Waste Form Development (MRWFD) Campaign Off-gas Sigma Team has performed research and development on iodine control and iodine waste forms for the past several years. This research and development has included iodine adsorption tests using a laboratory-scale test system containing multiple-segmented fixed beds of iodine adsorbents. Iodine capture performance has been tested using (a) non-radioactive synthetic gas mixtures blended from air, nitrogen, NO, NO_2, water, to simulate dissolver off-gas (DOG) and vessel off-gas (VOG) streams from used nuclear fuel aqueous reprocessing, (b) inorganic and organic iodine species, and (c) different sorbents.

An initial test of silver-functionalized mordenite in polyacrylonitrile matrix (AgZ-PAN) was conducted to assess if this sorbent, initially designed for selective sorption of Xe that evolves into used fuel reprocessing off-gas streams, could also be a candidate for iodine sorption. This test was conducted using the same deep-bed test system and methodologies used in many prior iodine sorption tests using other sorbents. Diatomic iodine (I_2) was used as the target iodide in a gas stream containing air, NO, NO_2, and moisture designed to simulate an aqueous reprocessing dissolver off-gas (DOG) stream.

The test demonstrated that the AgZ-PAN can capture iodine to provide decontamination factors between 2,000-10,000 prior to breakthrough of the sorbent bed. The maximum chemisorption capacity depends on the relative Ag content compared to other Ag-containing sorbents; but furthermore, only about 50% iodine utilization was achieved, compared to AgZ and Ag Aerogel, which can achieve near 100% Ag utilization if those sorbents are chemically reduced to produce the highest Ag reactivity. Perhaps the AgZ-PAN could also be chemically reduced to improve its Ag utilization.

But a further consideration is the amount of Ag that appears to not chemisorb via reaction with the Ag, but appears to sorb onto the polyacrylonitrile moiety. This iodine appears to desorb under air purging conditions, and presents a risk of iodine release from spent AgZ-PAN if it were to be used for an iodine sorbent. Furthermore, while investigations have been in progress for years to evaluate the so-far promising capability of using the AgZ or AgAero sorbents in an eventual iodine waste form, the presence of the acrylonitrile moiety, which may also contain weakly held iodine, may affect the use of AgZ-PAN in an iodine waste form. A possible alternative use of AgZ-PAN would be to take advantage of the ability to release iodine upon purging to enable regeneration of the AgZ-PAN for multiple iodine sorption cycles. In this case, the impact of chemisorbed iodine, reacted with the silver and so not easily regenerable, along with how to trap and manage the iodine that does desorb, would need to be considered.

These results also indicate that if AgZ-PAN is used for Xe capture, it would also capture, with high efficiencies (up to the point of sorbent breakthrough), any iodine that is present in the off-gas stream at the point of Xe capture. Possible benefits (such as more efficient iodine capture, or perhaps use as an iodine polishing filter), and possible other consequences (such as contamination by I-129 of spent AgZ-PAN, and possible interference by iodine with Xe capture), would need to be considered for use of AgZ-PAN for Xe capture.

Page intentionally left blank

ACKNOWLEDGEMENTS

The authors acknowledge others who helped guide or perform this iodine adsorption test. Jack Law of the Idaho National Laboratory provided programmatic and technical direction. Meghan Fujimoto provided testing and sampling support. Sample analyses were performed by Duane Ball in the INL Chemistry and Radiation Measurement Department, and Megha Dubey of the INL Center for Advanced Engineering Studies.

Page intentionally left blank

CONTENTS

SUMMARY iii

ACKNOWLEDGEMENTS v

ACRONYMS ix

1. INTRODUCTION 1

2. DEEP BED IODINE SORBENT TEST SYSTEM 1
   - 2.1 Process Gas Supply System 3
   - 2.2 Sorbent Bed Segments 3
   - 2.3 Sample Collection and Analysis 4

3. AgZ-PAN IODINE SORPTION TEST RESULTS 5
   - 3.1 Gaseous Measurements, Iodine DFs, and MTZ 6
   - 3.2 Sorbent Loading, Capacity, Silver Utilization 7
   - 3.3 Post-Test Purging 10

4. CONCLUSIONS 11

5. REFERENCES 12

FIGURES

Figure 2-1. Deep-bed adsorption test system. 2

Figure 2-2. Deep-bed adsorption test system inside a laboratory hood. At left: Oven containing the sorbent beds; and middle showing a 100-mL gas scrubbing impinger, and glass sample tube for GC analysis. At right: Thermal control panels on permeation tube oven and humidifier water bath. 2

Figure 2-3. Air supply polishing filters for halogens, hydrocarbons, and moisture 3

Figure 2-4. Configuration of the sorbent beds inside the temperature-controlled oven 4

Figure 3-1. AgZ-PAN prior to testing in the five sorbent bed segments (left), midway during the test (middle), and after the test end (right) 6

Figure 3-2. Iodine DF trends over time for Test AgZ-PAN-1 I2. 7

Figure 3-3. Bed segment outlet I_2 concentration trends over time for Test AgZ-PAN-1 I2. 7

Figure 3-4. Sorbent bed iodine concentrations for Test AgZ-PAN-1 I2. 8

Figure 3-5. Sorbent bed iodine concentrations versus time for Test AgZ-PAN-1 I2. 8

Figure 3-6. Sorbent bed Ag utilization versus time for Test AgZ-PAN-1 I2. 9

Figure 3-7. AgZ-PAN-1 I2 post-test sorbent purge results. 11

TABLES

Table 3-1. Results of the AgZ-PAN iodine sorption test. 5
Table 3-2. Sorbent bed composition after 76.2 test hours. 9
Table 3-3. Sorbent bed composition after 164 test hours. 10
Table 3-4. Sorbent bed composition at test end and after air purging (213.5 test hours). 10

ACRONYMS

AgZ	silver zeolite
AgZ-PAN	silver-functionalized mordenite in polyacrylonitrile matrix
DF	decontamination factor
DL	detection limit
DOE	Department of Energy
DOG	dissolver off-gas
EDS	energy dispersive spectroscopy
GC	gas chromatograph
GCMS	gas chromatography with mass spectrometry
ICPMS	inductively coupled plasma mass spectrometry
INL	Idaho National Laboratory
MRWFD	Material Recovery and Waste Form Development
MTZ	mass transfer zone
ppmv	parts per million by volume
SEM	scanning electron microscopy
VOG	vessel off-gas

Page intentionally left blank

Iodine Sorption on AgZ-PAN

1. INTRODUCTION

The Department of Energy (DOE) Nuclear Fuel Cycle and Supply Chain Program Material Recovery and Waste Form Development (MRWFD) Campaign Off-gas Sigma Team has performed research and development on iodine control and iodine waste forms for the past several years. This research and development has included iodine adsorption tests using a laboratory-scale test system containing multiple-segmented fixed beds of iodine adsorbents. Iodine capture performance has been tested using non-radioactive synthetic gas mixtures blended from air, nitrogen, NO, NO_2, water, to simulate dissolver off-gas (DOG) and vessel off-gas (VOG) streams from used nuclear fuel aqueous recycling. Testing has been done using iodine compounds that represent inorganic iodine (diatomic iodine I_2), and organic iodides (methyl iodide and butyl iodide).

Tests have been done using several candidate iodine sorbents including silver-laden sorbents silver-exchanged zeolite (AgZ, also called silver mordenite), and silver functionalized silver Aerogel. The presence of silver enables chemisorption of the iodine according to such possible overall chemical reactions as $Ag + I = AgI$ and $Ag + I + 3O = AgIO3$. Many prior tests dating back over decades have demonstrated iodine capture using silver-laden sorbents.

A silver-functionalized mordenite in polyacrylonitrile matrix (AgZ-PAN) sorbent has been developed at Idaho National Laboratory (INL) primarily for its ability to selectively capture Xe in used fuel reprocessing off-gas streams. Since this sorbent also contains Ag and is manufactured to have a high surface area, it has been proposed that this sorbent also be considered for iodine capture.

This report provides results of an initial test using AgZ-PAN to capture iodine. Diatomic iodine (I_2) was used as the target iodide in a gas stream containing air, NO, NO_2, and moisture designed to simulate an aqueous reprocessing dissolver off-gas (DOG) stream.

2. DEEP BED IODINE SORBENT TEST SYSTEM

Figure 2-1 shows a process diagram for the iodine test system. This is the same test system used in many other prior iodine sorption tests over the past 12 years, including the most recently completed organic iodide testing (Soelberg 2021). Figure 2-2 shows the main components inside a laboratory hood. The test system consists of the following main components:

- Process gas supply and blending system, which supplies gases from building compressed air, gas cylinders, gas generators, and a humidifier.
- Multiple sorbent bed system inside a heated oven.
- Process gas bypass.
- Inlet and bed segment outlet gas sampling system.

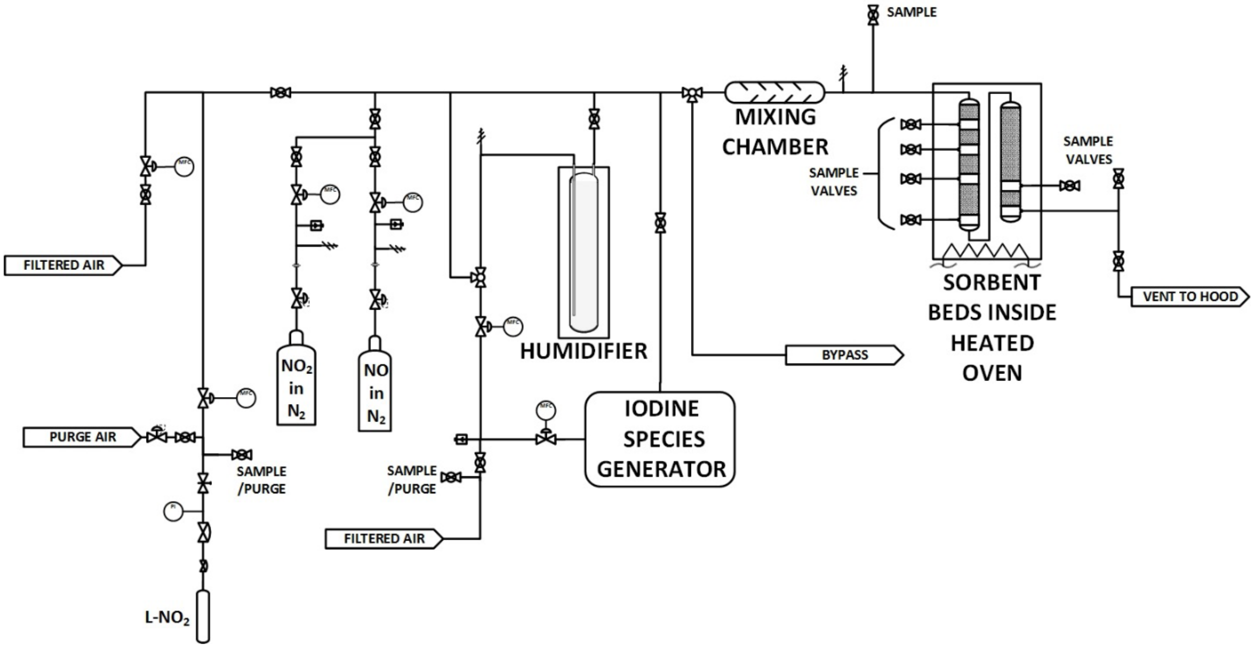

Figure 2-1. Deep-bed adsorption test system.

Figure 2-2. Deep-bed adsorption test system inside a laboratory hood. At left: Oven containing the sorbent beds; and middle showing a 100-mL gas scrubbing impinger, and glass sample tube for GC analysis. At right: Thermal control panels on permeation tube oven and humidifier water bath.

2.1 Process Gas Supply System

The simulated DOG gas mixture supply system for this test consists of air with a nominal moisture dewpoint of about 11°C, with a target 25 ppmv I_2 concentration. The moisture dewpoint was achieved by using the humidifier to add some moisture to the otherwise “dry” air supplied by the air supply system. Additional test conditions specified in the test plan vary in moisture content, organic iodide species, and concentration.

Air was supplied from the building compressed air system. This air is filtered for moisture, particulate matter, and hydrocarbons. In addition, a polishing filter system shown in Figure 2-3 includes silver mordenite sorbent to scrub halogens, activated charcoal for hydrocarbon scrubbing, and a combined mole sieve and silica gel sorbent for moisture scrubbing. The moisture scrubber changes color to indicate when the moisture scrubbing capacity is depleted. Frequent analysis of the sorbent bed inlet gas stream confirmed the hydrocarbon and iodine purity of the gas stream.

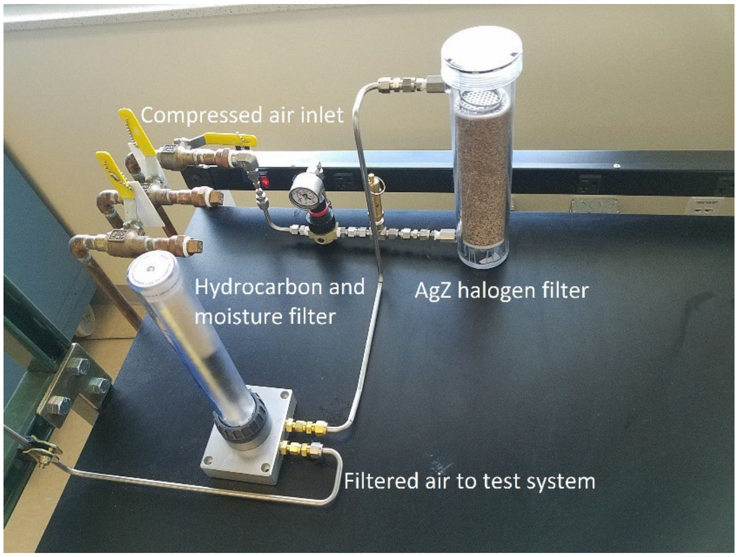

Figure 2-3. Air supply polishing filters for halogens, hydrocarbons, and moisture.

The I_2 was generated from calibrated semi-permeable tubes in a permeation tube system that maintains the permeation tubes at the temperature needed to provide the calibrated gas flowrate. The tubes (up to two), from VICI Metronics, were placed inside a Dynacalibrator Model 190 constant temperature permeation tube system also from VICI Metronics. The I_2 passes through the walls of the semipermeable tubes at calibrated rates determined by the oven temperature, and is carried away with a controlled flow of sweep air.

The sweep air and I_2 were blended in a mixing chamber upstream of the sorbent beds. All process lines that contain the blended gases were electrically heat traced to heat these lines and the mixed gas up to the target sorbent bed temperature.

2.2 Sorbent Bed Segments

Figure 2-4 shows how the sorbent beds are configured in a temperature-controlled oven. The current test design includes five sorbent bed segments. The sorbent bed segments are made of borosilicate glass with a glass frit at the bottom of each bed segment to support the granular sorbent. The gas flow was downward through the beds, to prevent any agitation of the bed particles in the event of high gas flows.

Figure 2-4. Configuration of the sorbent beds inside the temperature-controlled oven.

2.3 Sample Collection and Analysis

The gas stream can be sampled for analysis at the inlet to the sorbent beds, and at the outlet of each bed segment. Since the gas flowrate is essentially the same at all five sample locations, the removal efficiencies for the sorbent in all four beds can be determined by measuring the iodine gas species concentrations at these locations. The removal efficiency and decontamination factor for a bed segment or combination of bed segments can be calculated using the inlet and outlet iodine species concentrations.

When the gas stream is sampled, the entire gas stream is passed through impingers (for iodine scrubbing and analysis) or through sample tubes for gas chromatography (GC) analysis (for organic iodide analysis). The downstream sorbent beds are bypassed during gas sampling. The lost operating time for the downstream beds is tracked and recorded.

The iodine loadings on the sorbent and silver utilizations are determined by measurement of silver and adsorbed iodine concentrations using analytical methods such as scanning electron microscopy energy dispersive spectroscopy (SEM/EDS) or using wet chemistry methods of sorbent digestion followed by sample analysis.

For measuring the gaseous iodine concentration, the entire gas stream at any of the sample locations is passed through 100-mL impingers that contain 0.1 M NaOH for scrubbing halogen gases, including I_2 and HI, if present. The scrub solution pH was checked to ensure high pHs (>10) were maintained. This technique is modeled after EPA Method 26 (Determination of Hydrogen Halide and Halogen Emissions from Stationary Sources, Non-Isokinetic Method, EPA 2017). The caustic solution scrubs the halogens by hydrolyzing halogen gases to form a proton (H^+) and hypohalous acid.

Any HI, if present, dissociates into the caustic solution, and is included with I_2 in the analysis. This test method does not discriminate between I_2 and HI or other iodine species that are soluble in 0.1 M NaOH.

The bubbler solutions are analyzed by inductively coupled plasma mass spectrometry (ICPMS) per EPA SW-846 Method 6020A (EPA 2015). The gaseous iodine detection limit (DL) is about 0.1-1 ppb with this method, depending on dilution during analysis. Higher-concentration samples for gas streams with 1 ppb or higher iodine concentrations are typically diluted for analysis.

3. AgZ-PAN IODINE SORPTION TEST RESULTS

Table 3-1 summarizes results of this test. This table shows the test conditions including simulated DOG composition, flowrate, adsorption temperature, superficial gas velocity, sorbent bed depths, and gas residence times. The cumulative test duration was 212 hours, long enough to enable approximation of the capacity of the sorbent for iodine, and the mass transfer zone.

The sorbent used in this test was AgZ-PAN manufactured and provided by INL. Post-test silver concentrations in this sorbent for this test measured by SEM/EDS ranged between 5.0-6.3 wt% Ag.

Table 3-1. Results of the AgZ-PAN iodine sorption test.

Run Number	**AgZ-PAN-1 I2**
Simulate what off-gas?	DOG
Sorbent	AgZ-PAN
Ag concentration in sorbent from SEM/EDS, wt%	6.3
Temperature, deg. C	150
Total gas flowrate, L/min	1.69
Gas composition	11 deg. C dewpoint air
Target bed inlet CH3I conc., ppmv	25 ppmv I2
Average measured bed inlet I2 conc, ppmv	24.4
H2O conc, %	1.5
Sorption gas supercial velocity, m/min	10.0
Initial depths of each successive sorbent bed, inches	0.50, 1.00, 1.50, 3.50, 1.00
Cumulative initial sorbent bed depths, inches	0.50, 1.50, 3.00, 6.50, 7.50
Bed 1 out residence t, sec	0.08
Bed 2 out cumulative residence t, sec	0.23
Bed 3 out cumulative residence t, sec	0.46
Bed 4 out cumulative residence t, sec	0.99
Bed 5 out cumulative residence t, sec	1.14
Cumulative run time, hrs	212
Max test-end iodine loading from SEM/ED, wt%	4.78 wt%
Max test-end Ag utilization from SEM/EDS, %	64%
Maximum DF before breakthrough	2,000-10,000
Mass transfer zone depth, inches	4.5-6 in.

[iodine data 23sept21.xlsx]2017-21 summary

Figure 3-1 shows the sorbent in the beds prior to adsorption testing. The virgin sorbent was in the form of mainly tan-colored beads of varying sizes. A few of the beads are darker brown-colored. brownish pellets. Midway through the test, and by the test end, the sorbent in all five beds turned a darker reddish-purple color. Pure AgI has a yellow color, so this color change may have been due to sorption of iodine in the polyacrylonitrile. Pure iodine has a violet color, so perhaps some iodine is retained in or has stained the polyacrylonitrile. This darkening of the sorbent has not occurred on AgZ during many prior

AgZ iodine sorption tests, in which test results have shown little if any measureable sorption of iodine on the zeolite.

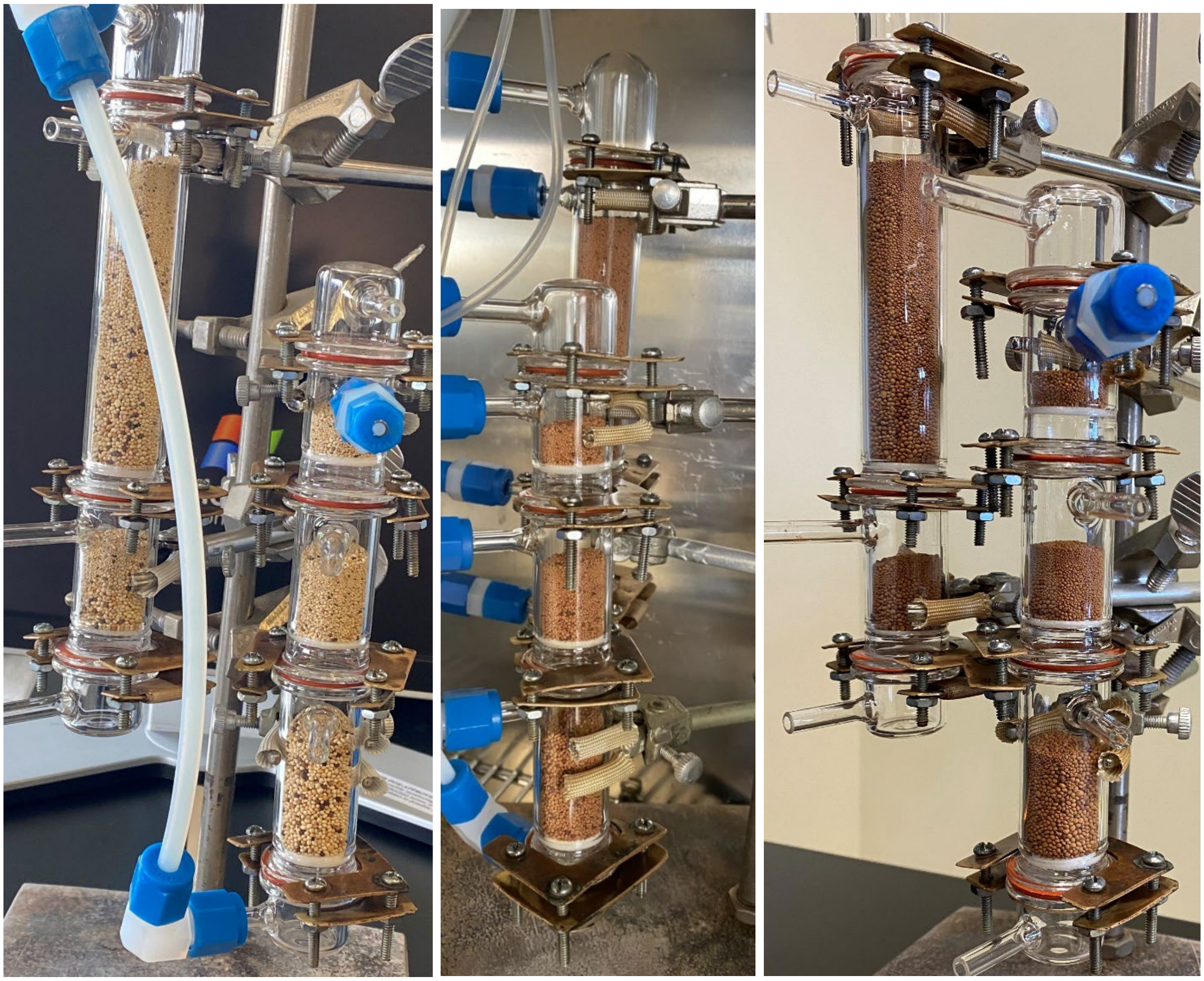

Figure 3-1. AgZ-PAN prior to testing in the five sorbent bed segments (left), midway during the test (middle), and after the test end (right).

3.1 Gaseous Measurements, Iodine DFs, and MTZ

Figure 3-2 shows the measured decontamination factors (DFs) during this test. The DF is the ratio of the amount of total iodine measured in the bed inlet gas to the amount of total iodine measured in the bed outlet gas. Its relationship to the removal efficiency is:

DF = 100/(100-removal efficiency %)

This figure shows that the maximum DFs ranged from about 2,000-10,000 before breakthrough (as defined when the DF begins to rapidly decrease, eventually decreasing to about 1). As expected, the 0.5 inch deep Bed 1 had broken through even before the first sample could be taken at under 0.2 hr. The Bed 1 outlet DF decreased most rapidly, approaching 1 after only about 20 hours of operation. The Bed 2 DF decreased next from about 2,000 at about 20 test hours to about 1 by about hour 50. Bed 2, with a total bed depth of 1.5 inches including Bed 1, was so shallow that it was within the estimated depth of the MTZ within the first 20 test hours.

Bed 3, with a cumulative depth (including beds 1 and 2) of 3.0 inches, reached breakthrough at about hour 30, when the DF dropped from almost 4,000 to about 1 by hour 50. The Bed 4 and 5 DF trends were close, because the Bed 5 depth added only 1 inch to the cumulative Bed 4 depth of 6.5 inches. The DFs for these beds ranged from above 10,000 to about 4,000 just prior to breakthrough at about hour 50. Both Bed 4 and Bed 5 reached saturation, with a DF of about 1, by about hour 100. During the remaining ½ of the 212 hour test, the DF was essentially 1, and essentially no iodine was sorbed because all 5 beds had approached the sorbent capacity.

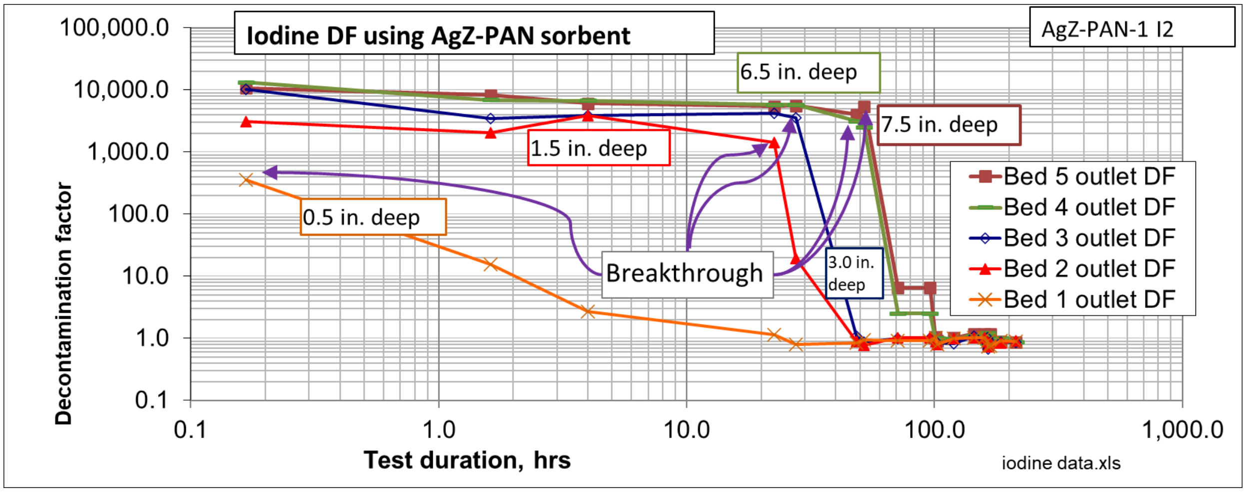

Figure 3-2. Iodine DF trends over time for Test AgZ-PAN-1 I2.

This same trend of bed-by-bed breakthrough and saturation is shown in Figure 3-3. The gas-phase bed outlet I_2 concentrations are graphically a mirror image of the DFs. In succession and at the same test times of bed breakthrough and saturation, the bed outlet I_2 levels increased from about 0.003-0.01 ppmv prior to breakthrough to eventually match the bed inlet concentration, when no more iodine could be sorbed.

As the MTZ progressed through the total depth of all bed segments during this test, the MTZ depth ranged from about 4.5-6 inches based on these gaseous measurements.

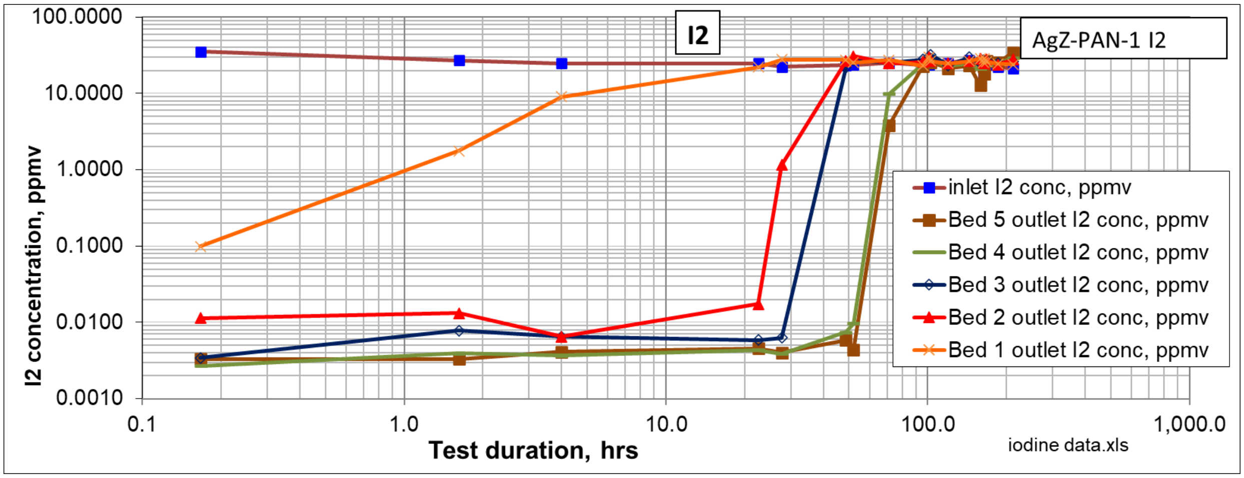

Figure 3-3. Bed segment outlet I_2 concentration trends over time for Test AgZ-PAN-1 I2.

3.2 Sorbent Loading, Capacity, Silver Utilization

Iodine loading on the sorbent was measured twice during the test (at hours 76 and 164) and after the test ended and the sorbent was purged. Figure 3-4 shows the trend of iodine loadings on the sorbent during the test duration. These measurements were made by SEM/EDS. In order to obtain representative average analyses, spent sorbent samples were ground to a very fine particle size before mounting for analysis. The samples were gold, not carbon, coated in order to obtain an estimate of the carbon levels in the samples (recognizing that EDS measurement of elements with atomic weights as low as carbon are not high quality). Since these samples were not mounted in epoxy, cut, ground, and polished, the numerical accuracy of the EDS analyses is subject to particle and surface variations. The analysis results are not more accurate than about +/-10% of values greater than 1 wt%.

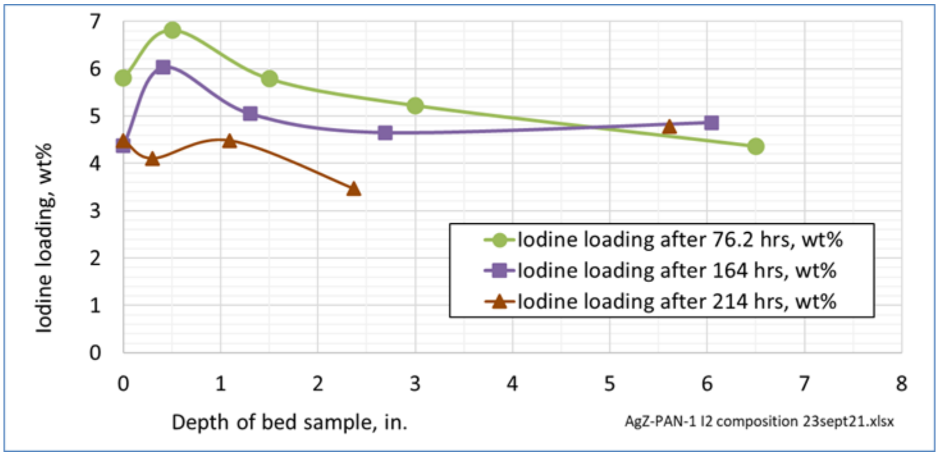

Figure 3-4. Sorbent bed iodine concentrations for Test AgZ-PAN-1 I2.

The variability of the EDS is a result of the limited accuracy of the EDS measurements. At hour 76, Beds 1-3 appear to have relatively similar iodine concentrations, consistent with gas-phase analyses that indicate these beds had already reached their sorption capacities. The beds 4 and 5 have iodine levels almost as high as beds 1-3, consistent with the gas-phase measurements that show that beds 4 and 5 had broken through but not yet reached their capacity. The iodine levels for the 164-hr and 214 hr (post-test and post air-purge) suggest that by those times, the sorbent capacity had been reached in all five beds.

Figure 3-5 shows the sorbent iodine concentrations versus time. For each bed sample time, the iodine concentrations for each bed, and for the average of beds that had reached saturation, are shown. The average values indicate that after hour 76, and especially after the test and after post-test air purging to remove weakly-held iodine, iodine concentrations actually decreased. This is further discussed in the next section.

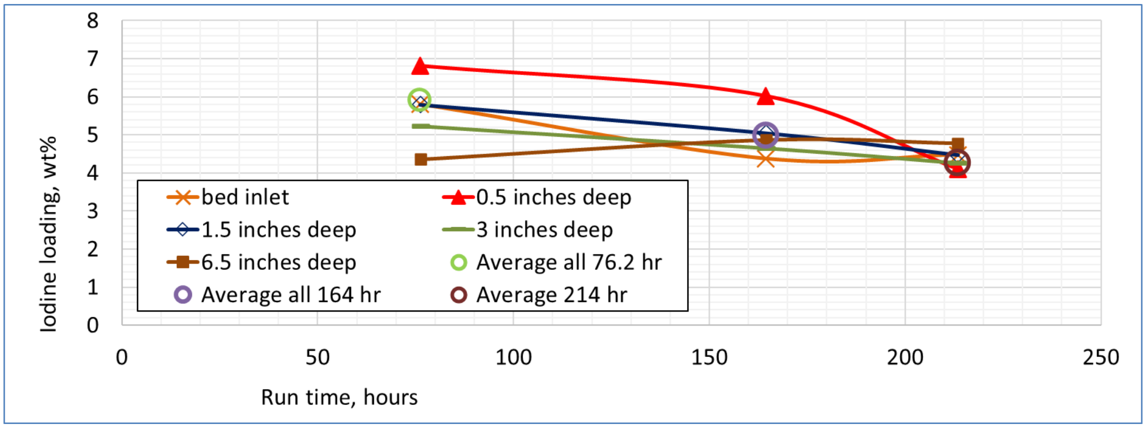

Figure 3-5. Sorbent bed iodine concentrations versus time for Test AgZ-PAN-1 I2.

Figure 3-6 shows the sorbent Ag utilization efficiencies over time, assuming the formation of either AgI or $AgIO_3$ from chemisorption. This figure has the same shape as the prior figure, and shows that iodine levels corresponded to Ag utilization that averaged as high as about 80% for the hour 76 samples (for the sorbent beds that reached saturation); decreased to about 70% for the hour 164 samples; and decreased to about 58% for the hour 214 (post-test, post-purge) samples. This is further discussed in the next section.

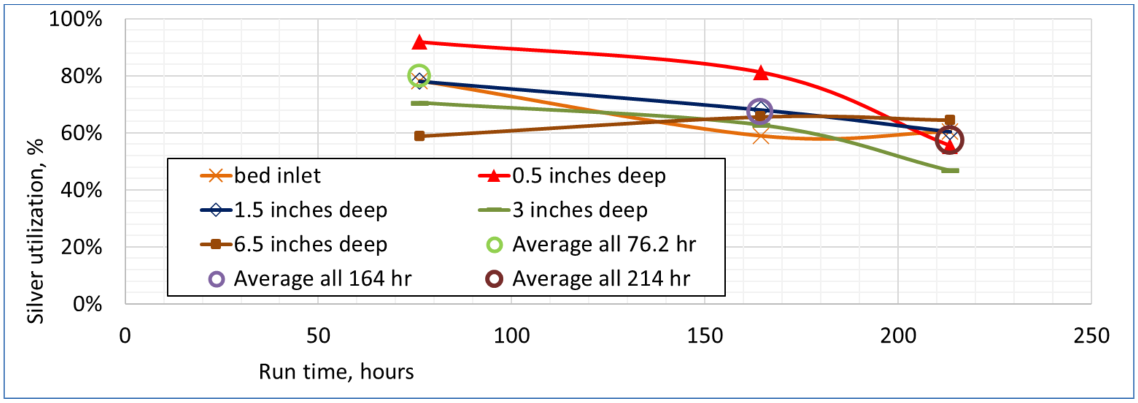

Figure 3-6. Sorbent bed Ag utilization versus time for Test AgZ-PAN-1 I2.

The source data for these figures is shown in Tables 3-2, 3-3, and 3-4. The iodine mass balance closure was 104% up until all five beds reached their sorbent capacity. After that (by about hour 100) iodine was no longer measurably captured in the five beds.

Table 3-2. Sorbent bed composition after 76.2 test hours.

Element	Sorbent composition, wt% after 76.2 hours					Avg or total, wt% or in.	Std dev, % of avg
	Bed 1	Bed 2	Bed 3	Bed 4	Bed 5		
C	17.58	16.55	19.27	18.73	20.83	18.59	8.8%
N	9.50	9.50	9.50	9.33	9.71	9.51	1.4%
O	30.94	30.18	30.80	35.64	36.53	32.81	9.2%
Na	1.46	1.31	1.22	1.72	2.00	1.54	20.7%
Mg	0.00	0.00	0.00	0.07	0.25	0.06	170.5%
Al	3.72	3.66	3.50	3.36	3.24	3.49	5.8%
Si	24.49	24.28	23.12	19.84	17.80	21.91	13.5%
Ag	6.45	7.62	6.73	5.91	5.06	6.35	15.0%
K	0.00	0.02	0.00	0.10	0.10	0.04	122.0%
Ca	0.00	0.00	0.00	0.00	0.03	0.01	223.6%
I	5.80	6.82	5.79	5.23	4.36	5.91	---
Fe	0.07	0.08	0.07	0.08	0.09	0.08	11.4%
Sum	100.00	100.00	100.00	100.00	100.01	100.23	
Starting incremental depth, in.	0.50	1.00	1.50	3.50	1.00	7.50	
Starting cumulative depth at top of bed, in.	0.00	0.50	1.50	3.00	6.50	6.50	
Starting bed mass, g	1.55	2.88	4.27	10.65	2.99	22.3	
Iodine adsorbed, g	0.106	0.167	0.223	0.465	0.130	1.091	
Cumulative iodine adsorbed plus losses, g	0.106	0.167	0.223	0.465	0.130	1.091	
Ag utilization, %	78.3%	92.0%	78.1%	70.5%	58.87%	79.7%	

Cumu-lative iodine fed, gm	Iodine MB closure
1.05	104%

Table 3-3. Sorbent bed composition after 164 test hours.

	Sorbent composition, wt% after 164 hours						
Element	Bed 1	Bed 2	Bed 3	Bed 4	Bed 5	Avg or total, wt% or in.	Std dev, % of avg
C	20.71	15.21	17.68	19.72	18.31	18.33	11.5%
N	9.24	8.59	8.88	9.15	9.13	9.00	2.9%
O	36.87	36.09	36.48	36.81	37.30	36.71	1.2%
Na	2.10	1.58	1.98	1.98	1.77	1.88	11.0%
Mg	0.28	0.00	0.21	0.20	0.10	0.16	68.7%
Al	3.27	3.55	3.51	3.30	3.31	3.39	3.9%
Si	17.90	22.08	19.97	18.68	19.31	19.59	8.1%
Ag	5.04	6.67	6.00	5.28	5.72	5.74	11.1%
K	0.09	0.08	0.10	0.09	0.10	0.09	7.5%
Ca	0.03	0.00	0.03	0.03	0.00	0.02	91.6%
I	4.37	6.03	5.05	4.65	4.86	4.99	---
Fe	0.09	0.11	0.11	0.12	0.08	0.10	13.9%
Sum	100.00	100.00	100.02	100.01	0.00	100.01	
Starting incremental depth, in.	0.41	0.90	1.39	3.35	0.90	6.94	
Starting cumulative depth at top of bed, in.	0.00	0.41	1.30	2.69	6.04	6.04	
Starting bed mass, g	1.27	2.57	3.94	10.21	2.68	20.67	
Iodine adsorbed, g	0.077	0.130	0.183	0.496	0.131	1.02	
Cumulative iodine adsorbed plus losses, g	0.093	0.151	0.202	0.520	0.144	1.11	
Ag utilization, %	59.0%	81.3%	68.1%	62.7%	65.6%	67.4%	

Table 3-4. Sorbent bed composition at test end and after air purging (213.5 test hours).

	Sorbent bed composition, wt% after 213.5 hours							
Element	Bed 1	Bed 2	Bed 3	Bed 4 top	Bed 4 mid	Bed 5	Avg or total, wt% or in.	Std dev, % of avg
C	20.16	20.90	20.16	25.00	21.07	20.02	21.22	9.0%
O	38.21	38.43	38.21	41.09	39.93	39.48	39.23	3.0%
Na	1.89	2.08	1.89	2.08	1.91	1.70	1.92	7.4%
Mg	0.06	0.15	0.06	0.21	0.08	0.04	0.10	63.2%
Al	3.94	4.00	3.94	3.44	3.77	3.80	3.82	5.4%
Si	23.86	23.32	23.86	19.04	22.11	22.60	22.46	8.1%
Ag	7.13	6.79	7.13	5.40	6.62	7.29	6.73	10.3%
K	0.11	0.13	0.11	0.15	0.15	0.15	0.13	13.2%
Ca	0.01	0.02	0.01	0.04	0.01	0.00	0.01	96.3%
I	4.48	4.11	4.48	3.47	4.26	4.78	4.26	---
Fe	0.13	0.08	0.13	0.08	0.09	0.14	0.11	24.7%
Sum	99.99	100.00	99.99	100.00	100.00	100.00	100.00	
Starting incremental depth, in.	0.30	0.79	1.28	3.25		0.78	6.39	
Starting cumulative depth at top of bed, in.	0.00	0.30	1.09	2.37		5.61	5.61	
Starting bed mass, g	0.87	2.09	3.48	9.71		2.00	18.15	
Iodine adsorbed, g	0.036	0.094	0.121	0.414		0.048	0.712	
Cumulative iodine adsorbed plus losses, g	0.066	0.134	0.157	0.452		0.079	0.887	
Ag utilization, %	60.4%	55.4%	60.4%	46.8%	57.5%	64.5%	57.5%	

3.3 Post-Test Purging

After the test, the sorbent beds were purged with dry air at the same temperature and gas flowrate conditions to desorb any amounts of iodine that may be loosely held or physisorbed. The purge results are shown in Figure 3-7. In the first hour of purging, the Bed 5 outlet gas iodine levels decreased from over 20 ppmv to 6 ppmv. Gaseous iodine levels continued to decrease by about three orders of magnitude over the next ~170 hours. During that time, a cumulative amount of about 34% of the sorbed iodine was desorbed into the purge gas. This decrease in sorbed iodine indicates that about 1/3rd of the sorbed iodine was not chemisorbed; and that Ag utilization values reported in the prior section, based on total sorbed iodine, over-estimate the true Ag utilization. The true Ag utilization was at most about 50%, about 2/3rd of the highest value of 80% reported in the prior section.

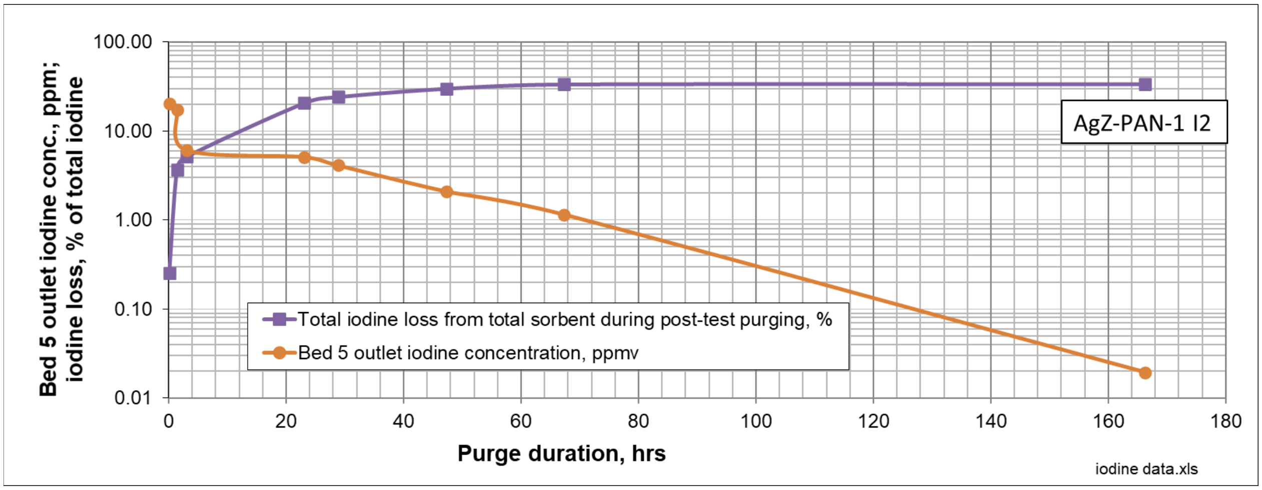

Figure 3-7. AgZ-PAN-1 I2 post-test sorbent purge results.

The decrease in the iodine capacity over time during the test, and especially between the last bed sample time of 164 hours and 214 hours (after the test end and post-test purging) is consistent with these purge results.

The decrease in iodine capacity due to iodine volatilization during purging is also consistent with the color change that appears due to iodine sorption on the polyacrylonitrile moiety of the sorbent, causing the color change from tan toward the characteristic purplish iodine color.

4. CONCLUSIONS

An initial test of AgZ-PAN was conducted to assess if this sorbent, initially designed for selective sorption of Xe that evolves into used fuel reprocessing off-gas streams, could also be a candidate for iodine sorption. This test was conducted using the same deep-bed test system and methodologies used in many prior iodine sorption tests using other sorbents.

The test demonstrated that the AgZ-PAN can capture iodine to provide decontamination factors between 2,000-10,000 prior to breakthrough of the sorbent bed. The maximum chemisorption capacity depends on the relative Ag content; but furthermore, achieves only about 50% iodine utilization, compared to AgZ and AgAero, which can achieve near 100% Ag utilization if those sorbents are chemically reduced to produce the highest Ag reactivity. Perhaps the AgZ-PAN could also be chemically reduced to improve its Ag utilization.

But a further consideration is the amount of Ag that appears to not chemisorb via reaction with the Ag, but sorbs onto the polyacrylonitrile moiety. This iodine appears to desorb under air purging conditions, and presents a risk of iodine release from spent AgZ-PAN if it were to be used for an iodine sorbent. Furthermore, while investigations have been in progress for years to evaluate the so-far promising capability of using the AgZ or AgAero sorbents in an eventual iodine waste form, the presence of the acrylonitrile moiety, which may also contain weakly held iodine, may affect the use of AgZ-PAN in an iodine waste form. A possible alternative use of AgZ-PAN would be to take advantage of the ability to release iodine upon purging to enable regeneration of the AgZ-PAN for multiple iodine sorption cycles. In this case, the impact of chemisorbed iodine, reacted with the silver and so not easily regenerable, along with how to trap and manage the iodine that does desorb, would need to be considered.

These results also indicate that if AgZ-PAN is used for Xe capture, it would also capture, with high efficiencies, any iodine that is present in the off-gas stream at the point of Xe capture. Possible benefits (such as more efficient iodine capture, or perhaps use as an iodine polishing filter), and possible other consequences such as contamination by I-129 of spent AgZ-PAN, and possible interference by iodine with Xe capture, would need to be considered for use of AgZ-PAN for Xe capture.

5. REFERENCES

EPA 2015. SW-846, "Test Methods for Evaluating Solid Waste, Physical/Chemical Methods," Method 6020A. Retrieved from epa.gov: https://www.epa.gov/sites/production/files/2015-07/documents/epa-6020a.pdf.

EPA 2017. Determination of Hydrogen Halide and Halogen Emissions from Stationary Sources, Non-Isokinetic Method. (2017, 8 2). 40 CFR 60, Appendix A.

Soelberg, Nick, Amy Welty, and Samuel Thomas, 2021, “Organic Iodine Capture from Vessel Off-gas,” INL/EXT-21-62077, March 2021.